THE JOURNAL OF PHYSICAL CHEMISTRY C
A JOURNAL OF THE AMERICAN CHEMICAL SOCIETY

pubs.acs.org/JPCC

Article

Role of Water Solvation on the Key Intermediates Catalyzing Oxygen Evolution on RuO_2

Giovanni Di Liberto,* Gianfranco Pacchioni, Yang Shao-Horn, and Livia Giordano*

Cite This: *J. Phys. Chem. C* 2023, 127, 10127−10133

Read Online

ACCESS | Metrics & More | Article Recommendations | Supporting Information

ABSTRACT: RuO_2 and IrO_2 are among the most active catalysts for the Oxygen Evolution Reaction (OER). Recently, it was demonstrated that the catalytic surface of these oxides plays a role in the reaction, where a hydrogen bond with a neighbor OH group stabilizes an unconventional −OO intermediate (−OO−H), prior to O_2 evolution. Quantum chemical calculations neglecting solvation effects indicated that this intermediate is more stable than the conventional −OOH, and that deprotonation of the stabilizing −OH is the rate limiting step for OER on RuO_2(110) and RuO_2(100). In this work, we investigate the role of water molecules on the relative stability of −OOH and −OO−H oxygenates on RuO_2 (110) by means of density functional theory calculations combined with ab initio Molecular Dynamics simulations (AIMD). We show that the two intermediates participate in a hydrogen bonding network with water to a similar extent, but leading to different interfacial water structures, with possible implications on interfacial proton dynamics and reaction kinetics. Moreover, −OOH can spontaneously convert to −OO−H through a process mediated by water, demonstrating the critical role of explicitly including water in the model. This study provides further mechanistic insights on the role of the oxide surface chemistry in the OER mechanism and highlights the importance of explicitly treating the catalyst/water interfaces including dynamical aspects to assess the stability and the interconversion mechanism of key surface species, since the adoption of static solvation approaches tends to overestimate the energetic difference between −OOH and −OO−H reaction intermediates.

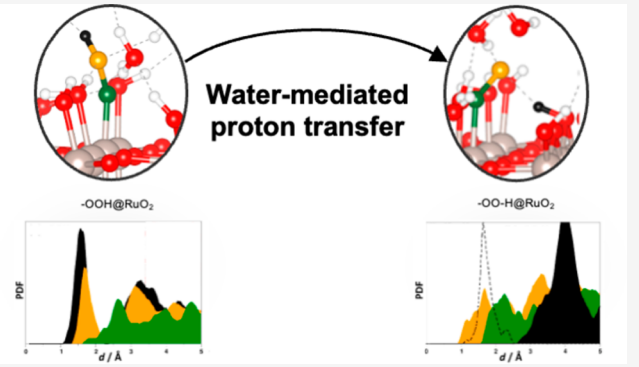

INTRODUCTION

Improving the efficiency of the oxygen evolution reaction (OER) is crucial for enabling the production of energy carriers such as hydrogen, ammonia, or synthetic fuels derived from CO_2 reduction.[1−3] In the case of water electrolysis, the cathodic part of an electrolyzer converts protons into molecular hydrogen and involves the formation of a single intermediate made by an adsorbed hydrogen atom on the active site of the catalyst,[4] so that the intermediate formation energy can be used as a suitable descriptor for the catalytic activity.[5,6] In the anodic part of the reaction the oxidation of water to molecular oxygen takes place, $2H_2O \rightarrow O_2 + 4H^+ + 4e^-$ in acid and $4OH^- \rightarrow O_2 + 2H_2O + 4e^-$ in alkaline solution. Such a reaction can be described by four concerted proton−electron transfer steps[7] as follows (in acid, where * denotes an active catalytic site):

$$H_2O + * \rightarrow OH^* + H^+ + e^- \quad (1)$$

$$OH^* \rightarrow O^* + H^+ + e^- \quad (2)$$

$$H_2O + O^* \rightarrow OOH^* + H^+ + e^- \quad (3)$$

$$OOH^* \rightarrow O_2 + * + H^+ + e^- \quad (4)$$

The best catalysts for water splitting are based on precious metal oxides (IrO_2 and RuO_2),[8,9] which display a significant overpotential for the OER.

An important aspect for understanding the reaction mechanism of an (electro)chemical reaction is the identification of the chemical intermediates,[10−12] since it can allow tailoring of the catalytic activity and rationally design novel systems with optimized performance. Specifically, it is of particular relevance to understand whether the catalytic surface plays a role in the reaction, resulting in the formation of unconventional intermediates.[13−16] Due to their record catalytic activity and stability in acid, a number of studies

Received: April 25, 2023
Revised: May 8, 2023
Published: May 18, 2023

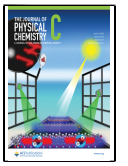

have investigated the OER reaction mechanism on RuO_2 and IrO_2.[14,15,17−20]

Recently, some of us have performed joint experimental and computational studies on RuO_2 single crystals with different crystallographic orientations.[17,18] Operando surface X-ray scattering crystal truncation rod (CTR) analyses combined with Density Functional Theory (DFT) calculations of RuO_2 surfaces as a function of the applied potential show an O−O intermediate adsorbed on Ru_{CUS} (−OO−H, Figure 1) at

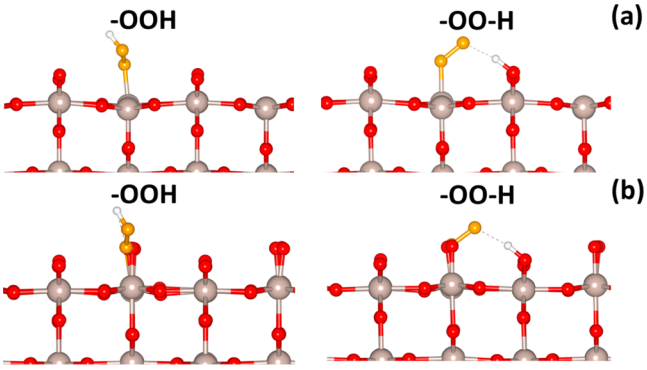

Figure 1. Structure of −OOH and −OO−H reaction intermediates adsorbed at the Ru_{CUS} site of the RuO_2 (110) surface. Panels (a) and (b) refers to stoichiometric and oxidized conditions. Ru atoms are represented in gray, surface oxygens in red, oxygens of −OOH and −OO−H reaction intermediates in orange and hydrogen in white.

potential 1.5 V_{RHE} which is stabilized by a hydrogen bond with a neighboring surface OH group. This surface complex is more stable than the conventional −OOH reaction intermediate on the undercoordinated Ru site (Figure 1a). This observation is further supported by other studies which reveal the higher stability of −OO−H compared to −OOH at the oxide/vacuum interface (dry conditions) on RuO_2.[17,18] Moreover, deprotonation of −OO−H represents the rate limiting step for OER on RuO_2(110) and RuO_2(100).[18] As pointed out by Divanis et al.,[21] the proton transfer to surface bridging oxygens, as observed in −OO−H, gives rise to a more favorable reaction pathway for OER which allows the DFT prediction to be reconciled with the high activity reported experimentally for RuO_2(110).[22] On the other hand, calculations with implicit solvent on IrO_2(110)[19] showed that −OOH spontaneously evolves to −OO−H through a direct proton transfer. Compared with previous studies performed in vacuum[17,18] or in implicit solvent,[19] the inclusion of water solvent in the computational model may imply relevant changes in the energetics and reactivity of the pre-OER surface intermediates.

In this work, we investigate the interplay between the water solvent and the catalytic surface in stabilizing the pre-OER reaction intermediates by studying the dynamics of the conventional −OOH and newly reported −OO−H intermediates on RuO_2(110) in an aqueous environment, thus considering explicitly the role of the solvent by means of DFT calculations in conjunction with ab initio molecular dynamics (AIMD). AIMD of −OOH and −OO−H surface complexes in the presence of water molecules show that the two species have a distinct chemical interaction with the solvent. Specifically, the −OO−H system is characterized by a rather stable chemical interaction between the −OO and H, where the presence of water does not alter the hydrogen bond between −OO and H species, indicating that the intermediate is suitable to form in water and can play a role in the OER. On the other hand, the presence of water enables that −OOH spontaneously interconverts to −OO−H via a process mediated by a water molecule, while −OO−H remains stable over time. The presence of the solvent is responsible for comparable stabilization of the two species, without altering the energetic ordering with respect to vacuum conditions, further validating previous work.[18] This result demonstrates the importance of the −OO−H species with respect to the conventional reaction intermediate, and the potential role of the solvent not only as a dielectric medium, where the reaction occurs, but also as a source of ligand molecules that can take part in the reaction. The adoption of static solvation schemes, consisting of small water clusters surrounding the reaction intermediate (micro-solvation), tends to overestimate the energetic difference between the two intermediates, showing that the complex surface chemistry of RuO_2 (110) requires the treatment of dynamical effects, where the surface can induce a sizable dissociation of adsorbed solvent molecules. Future work will be dedicated to the role of solvation in the chemistry of unconventional reaction paths for OER.

COMPUTATIONAL DETAILS

Density Functional Theory (DFT) calculations were performed using the VASP[44−46] code and the generalized gradient approximation, as implemented in the Perdew−Burke−Ernzerhof (PBE) functional.[47] Ab-initio Molecular Dynamics (MD) trajectories were propagated at a working temperature of 350 K, which guarantees a frank diffusive motion of liquid water,[31] and controlled by the Nosé−Hoover thermostat.[48,49] Full details on the computational setup and how the working simulation cells were created are reported in the Supporting Information.

The computational setup is consistent with that adopted in refs 17 and 18. A possible way to improve the description of the electronic structure of both RuO_2 and water is the adoption of hybrid functionals,[50−52] that however are computational demanding. Recently, a nonhybrid functional showed reasonable results,[31] including the PBE in conjunction with the Grimme's parametrization scheme (PBE+D3);[53−55] we have then decided to study the RuO_2/water interface with PBE+D3.[56]

RESULTS AND DISCUSSION

The attention of this work is on the relative stability of two key intermediates in the OER under different environments. One intermediate is a species generally assumed to form during this reaction, indicated here as −OOH, Figure 1a; the second is a novel species where a −OO group interacts via hydrogen bonding with a surface OH at the oxygen bridging site, indicated here as −OO−H, Figure 1b. We adsorbed −OOH and −OO−H species on the stoichiometric RuO_2 (110) surface, comprising two-coordinated bridging oxygen sites O_{2c} and empty coordinatively unsaturated Ru sites Ru_{CUS}. The Gibbs free energy of the intermediates, computed with respect to the reference free catalyst (empty Ru_{CUS} site) and water, in vacuum is 3.43 and 3.24 eV for −OOH and −OO−H respectively, indicating that the latter is more stable by 0.19 eV, as shown in Figure 1a. The two reaction intermediates are different in nature and are characterized by different charge transfers with the oxide. The −OOH intermediate has a O−O distance of 1.45 Å, typical of hydroperoxide OOH^- consistent

https://doi.org/10.1021/acs.jpcc.3c02733
J. Phys. Chem. C 2023, 127, 10127−10133

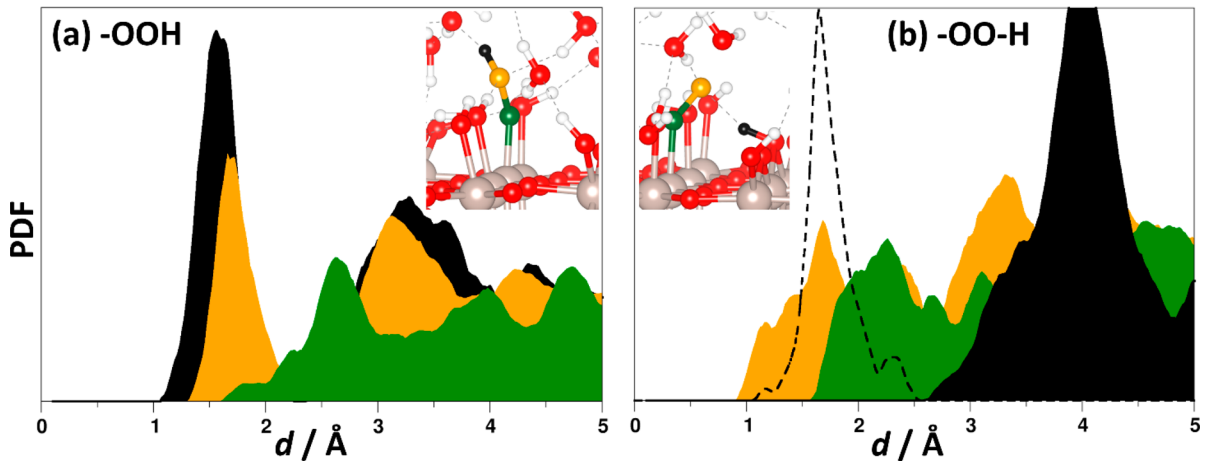

Figure 2. Radial distribution function between $-O_I-O_{II}-H$ atoms and water. O_I, O_{II}, and H atoms of −OOH and $-OO-H$ intermediates are reported in green, orange, and black, respectively. Panels (a) and (b) are for −OOH and $-OO-H$, respectively. Black, orange, and green lines are for $H-O_{H_2O}$ hydrogen bonding, $O_{II}-H_{H2O}$ bonding, and $O_I-H_{H_2O}$ hydrogen bonding. The dashed black curve in panel b is associated with the $O_{II}-H$ interaction of the $OO-H$ intermediate. Insets: structure of −OOH and $-OO-H$ reaction intermediates at the RuO_2/water interface. Ru atoms are represented in gray, surface oxygens in red, oxygens of −OOH and $-OO-H$ reaction intermediates in orange, and hydrogens in black.

with its negative charge (−0.3 |e| as estimated by the Bader charge).[23] Conversely, $-OO-H$ consists of a superoxo O_2^-, as demonstrated by the O−O distance (1.30 Å), and a proton adsorbed on the bridging oxygen site, and is then characterized by a lower interfacial charge transfer (0.1 |e|).

OER conditions could lead to oxidation of the electrode surface relative to that in vacuum, by filling the Ru_{CUS} sites by oxygen adsorbates.[17] To understand the effect of surface oxidation on the relative stability of −OOH and $-OO-H$, we repeated the simulation in the presence of an oxidized surface, as in previous work,[18] where every Ru_{CUS} on the top layer, except the one where −OOH or $-OO-H$ is adsorbed, is bound to an O atom, as shown in Figure 1b. The Gibbs free energies of the −OOH and $-OO-H$ intermediates become 3.72 and 3.11 eV, demonstrating that the latter intermediate is more stable than the classical −OOH species under these conditions by 0.61 eV, in agreement with previous work (0.54 eV).[18] On the other hand, the interfacial charge transfer between the intermediates and the surface is not affected by the oxidation of the surface, as demonstrated by the O−O distance in −OOH of 1.45 Å typical of a hydroperoxide, and the O−O distance of 1.30 Å in $-OO-H$, characteristic of a superoxo group. The destabilization of −OOH and stabilization of $-OO-H$ compared to the stoichiometric surface can be understood considering the lower reducing power of the oxidized surface which renders the formation of hydroperoxide less favorable, whereas it affects the stability of $-OO-H$ only slightly, due to its reduced interfacial charge transfer. Therefore, the oxidation of the surface does not lead to changes in the stability ranking of −OOH and $-OO-H$ and would only stabilize the $-OO-H$ intermediate. For this reason, we consider stoichiometric surface models in the following to study the interaction of water with oxygenate intermediates. We also checked that neglecting spin-polarization induces errors as high as 0.1 eV (see Table S2), which allows us to neglect spin-polarization and to reduce the computational cost of the simulations.

We then considered the effect of water molecules on the relative stability of −OOH and $-OO-H$. We propagated a trajectory of the RuO_2/H_2O interface made by a $(H_2O)_{69}$ water box, which ensures a water density close to 1 g·cm^{-3}. The initial configuration of the RuO_2/H_2O interface was made by water molecularly adsorbed on the surface. The system has been equilibrated for 1 ps. Interestingly, after propagating the trajectory for 2.5 ps, about 40% of water molecules on the surface dissociate, indicating a tendency of the RuO_2 (110) surface to induce water dissociation, in agreement with previous work on static water monolayers adsorbed on RuO_2(110).[24] This result is also consistent with previous MD reports,[20] showing that about 50% of water on the surface dissociate after very long propagation times. Although much larger simulations times are needed to reach a full sampling of the configurational space,[25,26] we can the propagation time in the present work acceptable for the specific purpose of describing the chemistry of the RuO_2 (110) surface. Further details on how the surface interacts with water as evinced by the analysis of the Pair Distribution Function (PDF) can be found in Section S3.

We now discuss the effect of the water layer on the stability of −OOH and $-OO-H$ intermediates. We propagated two different trajectories characterized by the presence of −OOH and $-OO-H$ intermediates adsorbed on the surface. The interaction network with the solvent is different for the two intermediates. In the case of −OOH, labeled as $O_IO_{II}H$, the O_I atom (bound to the surface) does not form any hydrogen bond with water, as shown by the PDF (Figure 2a), where its coordination number with Hydrogen atoms of water is less than 0.1. The O_{II} species, that is the O atom bound to H, and farthest from the RuO_2 surface, forms on average 1.5 hydrogen bonds with water. The hydrogen atom is always involved in a hydrogen bond with water, with a coordination number close to one (Figure 2a). Moving to the $-OO-H$ species, labeled as $-O_IO_{II}-H$, the PDF (Figure 2b) between O_I and water indicates that 0.5 hydrogen bonds are formed, different from O_I in −OOH. The O_{II} atom forms on average two hydrogen bonds, one with a water molecule and the second one with the H atom of the surface OH group. The H atom in turn does not interact with solvent molecules, as suggested by the calculated coordination number with O atoms of water (<0.1), since it is strongly linked to the O_IO_{II} species, having the calculated averaged $O_{II}-H$ distance of 1.6 Å. This result shows that the $-OO-H$ species is stable in the presence of water and its

https://doi.org/10.1021/acs.jpcc.3c02733
J. Phys. Chem. C 2023, 127, 10127−10133

dynamical behavior does not imply the breaking of the −OO−H hydrogen bond. It is interesting to observe that the first intermediate is involved in about 2.5 hydrogen bonds with water, which is consistent with previous reports demonstrating that OOH species on metals are surrounded by a micro-solvation environment made by three water molecules.[27] Remarkably, the interaction network of water is totally different for $-O_IO_{II}H$ and $-O_IO_{II}-H$ intermediates. In −OOH, O_{II} and H are mainly involved in 1.5 and 1 hydrogen bonds respectively, and O_I does not interact with water. In −OO−H, O_I is involved in 0.5 bonds, and O_{II} forms two bonds, one with H, and the other with a water molecule. The different water networks for the two reaction intermediates can have implications on the reaction kinetics involving these species. Indeed, as pointed out for the case of the hydrogen evolution reaction (HER), a more rigid water network might imply a larger reorganization energy,[28] and a slower transfer of species between the interfacial region and the bulk of the electrolyte.[29]

The contribution of the solvation energy was evaluated by sampling energy points of the −OOH and −OO−H trajectories. Given that very large simulation times are needed to properly sample the configurational space of complex system including water, we sampled a number of points leading to an acceptable error bar. The error was estimated by means of the blocking analysis.[30,31] We observed that a sampling of 2 ps (4000 structures) was sufficient to obtain an error of 0.1 eV, which we can consider leads to reasonable results. Having $\Delta G_{X/H_2O} = \Delta\tilde{G}_X - \Delta G_X$, where $\Delta G_{X/H_2O}$ is the stabilization contribution induced by the interaction of X (X = −OOH, −OO−H) with H_2O, $\Delta\tilde{G}_X$, and ΔG_X are the Gibbs free energies of the X in water and in vacuum, the contribution of solvation stabilizes both −OOH and −OO−H by $\Delta G_{-OOH/H_2O}$ = −0.42 eV and $\Delta G_{-OO-H/H_2O}$ = −0.28 eV respectively. These solvation energies are of the same order of magnitude as for other oxygenates species reported previously.[32] Then, it is possible to correct the Gibbs free energies with respect to those in vacuum as $\Delta\tilde{G}_X = \Delta G_{X,dry} + \Delta G_{X/H_2O}$. The calculated Gibbs free energies ($\Delta\tilde{G}_X$) of −OOH and −OO−H become 3.02 and 2.96 eV, respectively, from those in vacuum ($\Delta G_{X,dry}$), 3.43 and 3.24 eV, respectively. Because of the mentioned nearly systematic stabilization, the energy difference between the two intermediates is −0.06 eV, very similar to that found in vacuum (−0.19 eV). The limited effect of solvation on the relative stability of adsorbates is consistent with that reported for other intermediates on RuO_2 (110).[32,33] Of course, this result is affected by the rather low propagation time, and it must also be considered that such an energy difference is of the same order to the typical error of DFT calculations (0.1 eV). Therefore, it can be concluded that the two structures are nearly isoenergetic, justifying the predictions of previous work[18] in vacuum, where −OO−H is more stable than −OOH.

While the energy of the two intermediates is similar both in vacuum and in water, the dynamics behavior is different. When the trajectories of −OOH and −OO−H groups were propagated further, we observed that after one additional picosecond, −OOH spontaneously converts irreversibly into the −OO−H species. The −OO−H intermediate did not show any structural change. This result provides further evidence for the stability of this intermediate and, as a result, of its key role for OER. More importantly, the path is not simply described by a proton transfer according to the reaction $-OOH + O_{br} \rightarrow -OO-H-O_{br}$ (where O_{br} is a surface bridging oxygen), but the process is mediated by a water molecule via the formation of a H_3O^+ species, as depicted in Figure 3. The −OOH intermediate is very fluxional (Figure 3),

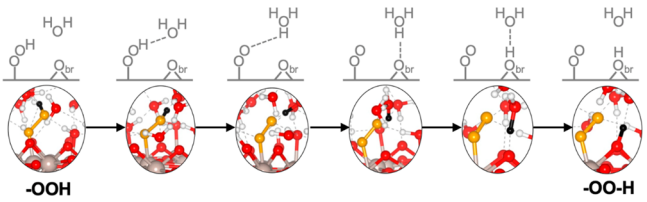

Figure 3. Schematic representation and snapshots of dynamics of −OOH interconversion to −OO−H. Ru atoms are represented in gray, surface and water oxygens in red, oxygens of −OOH and −OO−H reaction intermediates in orange, hydrogens of water in white, and hydrogens of −OOH and −OO−H reaction intermediates in black.

and the H atom of the −OOH complex is bound to a water molecule via hydrogen bonding. The H atom can even be transferred to the H_2O molecule, with formation of H_3O^+ (Figure 3), which in turn can share the proton with the O_{br} atom of the surface, leading finally to the formation of the $-OO-H-O_{br}$ adduct. This result shows that the presence of water does not affect the stability of the two intermediates which remains basically the same predicted in vacuum, but it mediates the transformation of the −OOH complex (if formed) to −OO−H via formation of H_3O^+ species. As discussed above, due to the different interfacial charge transfers of the two reaction intermediates, we expect surface oxidation to further increase the relative stability of the −OO−H intermediate. We notice that the explicit inclusion of water molecules and of dynamic effects is a step forward toward a realistic model of the electrochemical interface compared to calculations performed in vacuum. Other effects like the electric field due to the applied potential and the presence of ions in solution can also have a role, and their effect could be considered in future studies.

Once the important features of the RuO_2/water interface were established, as well as the chemistry of −OOH and −OO−H in water, we then investigated the performance of the state-the-art static approaches for the treatment of solvation of such species. Indeed, the simulation of explicit solid/water interfaces and the corresponding solvated intermediates is computationally demanding. This challenge has driven the development and adoption of affordable solvation approaches based on static calculations with a reduced number of solvent molecules. In this section, we compare the stability of −OOH and −OO−H species under different solvation schemes. In particular, we first considered a model consisting of a bilayer of water,[34−36] and then another model formed by three-water molecules, the so-called microsolvation scheme.[27] Moreover we also report and discuss the case of the smallest possible explicit solvation environment, represented by a single water molecule in section S4.

The first solvation scheme, a water bilayer, is a common choice for a static solvation environment, which has been used for instance for the case of metal surfaces, Pt electrodes in particular.[37−39] A possible limitation of this model is that the

https://doi.org/10.1021/acs.jpcc.3c02733
J. Phys. Chem. C 2023, 127, 10127−10133

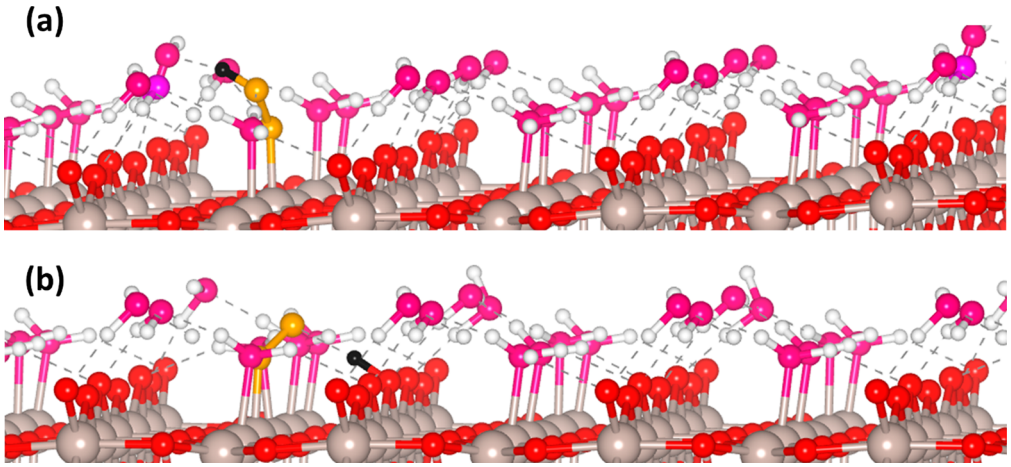

Figure 4. Panels (a) and (b) report the structure of −OOH and −OO−H adsorbed on RuO_2 (110) surface in the presence of an adsorbed water bilayer. Ru atoms are represented in gray, surface oxygens in red, water oxygen in pink, oxygens of −OOH and −OO−H reaction intermediates in orange, hydrogens of water in white, and hydrogens of −OOH and −OO−H reaction intermediates in black.

water bilayer must be commensurate with the lattice constants of the catalytic system, introducing possible strain effects. The structure of the two intermediates is reported in Figure 4. With this static solvation model, the calculated Gibbs free energies of −OOH and −OO−H intermediates are 3.95 and 3.06 eV. Thus, the order of stability is the same as that obtained with MD approaches, but the energy difference is much larger compared to the one obtained with MD probably due to the tendency of low dimensional and more rigid static solvation models to maximize the interaction between water and the reaction intermediate. The second static solvation model is based on the microsolvation approach recently proposed by Calle-Vallejo et al.[27] The basic idea is to approximate the entire solvation environment with a local one made by a few water molecules around the chemical intermediate. In this case, one must consider that small aggregates of water molecules can be characterized by several nearly isoenergetic local minima.[40−42] An optimum number of three molecules was found to nearly resemble the energy stabilization induced by an extended water bilayer.[27,43] Using this approach, the calculated free energies are 3.94 and 3.02 eV for −OOH and −OO−H, respectively, as shown in Figure S5. This result confirms that a microsolvation environment allows one to mimic the behavior of an extended water bilayer in stabilizing oxygenates. However, both the bilayer and microsolvation models exaggerate the difference in stability of the two isomers compared to the MD approach. Therefore, we conclude that molecular dynamics is essential to properly estimate the relative energy of two similar chemical intermediates, since the difference in stability can be overestimated using static approaches. This difference is probably due to the complex nature of the RuO_2/H_2O interface that requires accounting for the dynamics effects to properly describe the simultaneous presence of dissociated and molecularly adsorbed water molecules.

CONCLUSIONS

In this work we have investigated the interplay between the water solvent and the oxide surface in stabilizing OER reaction intermediates, focusing on the relative stability of −OOH and −OO−H species that can form on the RuO_2 (110) surface during the OER. These species are key intermediates in OER, but while the −OOH complex is usually assumed to be the only species present prior to O_2 evolution, the formation of −OO−H complexes has been suggested recently based on combined operando CTR measurements and theoretical studies.[17,18] These theoretical predictions have been done in vacuum conditions, leaving an open question on the stability and chemistry of the two complexes in aqueous environment. To this end, we have performed density functional theory in conjunction with *ab initio* molecular dynamics calculations. Our results show that the two species display very different chemistries when interacting with the solvent, resulting in different interfacial water structures with possible implications on the reaction kinetics. Moreover, solvation has a primary role in the conversion of the −OOH to −OO−H, via a dynamic process mediated by a water molecule. The second intermediate is stable along the simulation time explored here, and the −OO−H interaction remains intact during the simulation and is not broken by solvent molecules. These results demonstrate the importance and relevance of the −OO−H intermediate with respect to −OOH for OER on oxide catalysts. The inclusion of solvation implies a nearly systematic stabilization of both species, and does not alter the energetic ordering from vacuum conditions, thus justifying the predictions of ref 18. Finally, we have analyzed the performance of common static solvation schemes by using two well established static solvation approaches, the water bilayer and the microsolvation, finding that both lead to a considerable overestimation of the energy difference between the two species. In conclusion, this study provides an atomistic insight into the stability of the −OO−H OER reaction intermediate formed on the RuO_2(110) surface, compared to the conventional −OOH intermediate found for OER/ORR on metal surfaces, in an aqueous environment. It provides an important example of the interplay between the catalyst surface and the water solvent in stabilizing the reaction intermediates at the water/oxide interface, and of the need to explicitly include dynamical effects at water/solid interfaces.

ASSOCIATED CONTENT

Supporting Information

The Supporting Information is available free of charge at https://pubs.acs.org/doi/10.1021/acs.jpcc.3c02733.

https://doi.org/10.1021/acs.jpcc.3c02733
J. Phys. Chem. C 2023, 127, 10127−10133

Additional details related to computational models, extended RuO_2/water interface and static solvation schemes based on microsolvation. (PDF)

AUTHOR INFORMATION

Corresponding Authors

Giovanni Di Liberto − *Department of Materials Science, University of Milano-Bicocca, 20125 Milano, Italy;* orcid.org/0000-0003-4289-2732; Email: giovanni.diliberto@unimib.it

Livia Giordano − *Department of Materials Science, University of Milano-Bicocca, 20125 Milano, Italy;* orcid.org/0000-0002-6879-9424; Email: livia.giordano@unimib.it

Authors

Gianfranco Pacchioni − *Department of Materials Science, University of Milano-Bicocca, 20125 Milano, Italy;* orcid.org/0000-0002-4749-0751

Yang Shao-Horn − *Department of Materials Science and Engineering, Massachusetts Institute of Technology, Cambridge, Massachusetts 02139, United States; Department of Mechanical Engineering, Massachusetts Institute of Technology, Cambridge, Massachusetts 02139, United States;* orcid.org/0000-0001-8714-2121

Complete contact information is available at: https://pubs.acs.org/10.1021/acs.jpcc.3c02733

Notes

The authors declare no competing financial interest.

ACKNOWLEDGMENTS

We acknowledge the financial support by Cariplo Foundation. Access to the CINECA supercomputing resources was granted via ISCRAB. We also thank the COST Action 18234 supported by COST (European Cooperation in Science and Technology).

REFERENCES

(1) Gray, H. B. Powering the Planet with Solar Fuel. *Nat. Chem.* **2009**, *1* (1), 7−7.

(2) Andersen, S. Z.; Čolić, V.; Yang, S.; Schwalbe, J. A.; Nielander, A. C.; McEnaney, J. M.; Enemark-Rasmussen, K.; Baker, J. G.; Singh, A. R.; Rohr, B. A.; et al. I. A Rigorous Electrochemical Ammonia Synthesis Protocol with Quantitative Isotope Measurements. *Nature* **2019**, *570* (7762), 504−508.

(3) Liu, C.; Colón, B. C.; Ziesack, M.; Silver, P. A.; Nocera, D. G. Water Splitting-Biosynthetic System with CO 2 Reduction Efficiencies Exceeding Photosynthesis. *Science (1979)* **2016**, *352* (6290), 1210−1213.

(4) Nørskov, J. K.; Bligaard, T.; Logadottir, A.; Kitchin, J. R.; Chen, J. G.; Pandelov, S.; Stimming, U. Trends in the Exchange Current for Hydrogen Evolution. *J. Electrochem. Soc.* **2005**, *152* (3), J23.

(5) Nørskov, J. K.; Bligaard, T.; Rossmeisl, J.; Christensen, C. H. Towards the Computational Design of Solid Catalysts. *Nat. Chem.* **2009**, *1* (1), 37−46.

(6) Ulissi, Z. W.; Medford, A. J.; Bligaard, T.; Nørskov, J. K. To Address Surface Reaction Network Complexity Using Scaling Relations Machine Learning and DFT Calculations. *Nature Communications 2017 8:1* **2017**, *8* (1), 1−7.

(7) Giordano, L.; Han, B.; Risch, M.; Hong, W. T.; Rao, R. R.; Stoerzinger, K. A.; Shao-Horn, Y. PH Dependence of OER Activity of Oxides: Current and Future Perspectives. *Catal. Today* **2016**, *262*, 2−10.

(8) Lee, Y.; Suntivich, J.; May, K. J.; Perry, E. E.; Shao-Horn, Y. Synthesis and Activities of Rutile IrO 2 and RuO 2 Nanoparticles for Oxygen Evolution in Acid and Alkaline Solutions. *J. Phys. Chem. Lett.* **2012**, *3* (3), 399−404.

(9) Trasatti, S. Electrocatalysis in the Anodic Evolution of Oxygen and Chlorine. *Electrochim. Acta* **1984**, *29* (11), 1503−1512.

(10) Di Liberto, G.; Cipriano, L. A.; Pacchioni, G. Role of Dihydride and Dihydrogen Complexes in Hydrogen Evolution Reaction on Single-Atom Catalysts. *J. Am. Chem. Soc.* **2021**, *143* (48), 20431−20441.

(11) Cipriano, L. A.; Di Liberto, G.; Pacchioni, G. Superoxo and Peroxo Complexes on Single-Atom Catalysts: Impact on the Oxygen Evolution Reaction. *ACS Catal.* **2022**, *12*, 11682−11691.

(12) Zhong, L.; Li, S. Unconventional Oxygen Reduction Reaction Mechanism and Scaling Relation on Single-Atom Catalysts. *ACS Catal.* **2020**, *10* (7), 4313−4318.

(13) Liu, X.; Wang, Z.; Tian, Y.; Zhao, J. Graphdiyne-Supported Single Iron Atom: A Promising Electrocatalyst for Carbon Dioxide Electroreduction into Methane and Ethanol. *J. Phys. Chem. C* **2020**, *124* (6), 3722−3730.

(14) Zagalskaya, A.; Alexandrov, V. Role of Defects in the Interplay between Adsorbate Evolving and Lattice Oxygen Mechanisms of the Oxygen Evolution Reaction in RuO 2 and IrO 2. *ACS Catal.* **2020**, *10* (6), 3650−3657.

(15) Gauthier, J. A.; Dickens, C. F.; Chen, L. D.; Doyle, A. D.; Nørskov, J. K. Solvation Effects for Oxygen Evolution Reaction Catalysis on IrO 2 (110). *J. Phys. Chem. C* **2017**, *121* (21), 11455−11463.

(16) Wang, T.; Zhang, Y.; Huang, B.; Cai, B.; Rao, R. R.; Giordano, L.; Sun, S. G.; Shao-Horn, Y. Enhancing Oxygen Reduction Electrocatalysis by Tuning Interfacial Hydrogen Bonds. *Nat. Catal* **2021**, *4* (9), 753−762.

(17) Rao, R. R.; Kolb, M. J.; Halck, N. B.; Pedersen, A. F.; Mehta, A.; You, H.; Stoerzinger, K. A.; Feng, Z.; Hansen, H. A.; Zhou, H.; et al. Towards Identifying the Active Sites on RuO 2 (110) in Catalyzing Oxygen Evolution. *Energy Environ. Sci.* **2017**, *10* (12), 2626−2637.

(18) Rao, R. R.; Kolb, M. J.; Giordano, L.; Pedersen, A. F.; Katayama, Y.; Hwang, J.; Mehta, A.; You, H.; Lunger, J. R.; Zhou.; et al. Operando Identification of Site-Dependent Water Oxidation Activity on Ruthenium Dioxide Single-Crystal Surfaces. *Nat. Catal* **2020**, *3* (6), 516−525.

(19) Ping, Y.; Nielsen, R. J.; Goddard, W. A. The Reaction Mechanism with Free Energy Barriers at Constant Potentials for the Oxygen Evolution Reaction at the IrO 2 (110) Surface. *J. Am. Chem. Soc.* **2017**, *139* (1), 149−155.

(20) Creazzo, F.; Luber, S. Water-Assisted Chemical Route Towards the Oxygen Evolution Reaction at the Hydrated (110) Ruthenium Oxide Surface: Heterogeneous Catalysis via DFT-MD and Metadynamics Simulations. *Chem.—Eur. J.* **2021**, *27* (68), 17024−17037.

(21) Divanis, S.; Frandsen, A. M.; Kutlusoy, T.; Rossmeisl, J. Lifting the Discrepancy between Experimental Results and the Theoretical Predictions for the Catalytic Activity of RuO 2 (110) towards Oxygen Evolution Reaction. *Phys. Chem. Chem. Phys.* **2021**, *23* (35), 19141−19145.

(22) Kuo, D.-Y.; Paik, H.; Kloppenburg, J.; Faeth, B.; Shen, K. M.; Schlom, D. G.; Hautier, G.; Suntivich, J. Measurements of Oxygen Electroadsorption Energies and Oxygen Evolution Reaction on RuO 2 (110): A Discussion of the Sabatier Principle and Its Role in Electrocatalysis. *J. Am. Chem. Soc.* **2018**, *140* (50), 17597−17605.

(23) Blint, R. J.; Newton, M. D. *Ab Initio* Studies of Interoxygen Bonding in O_2, HO_2, H_2O_2, O_3, HO_3, and H_2O_3. *J. Chem. Phys.* **1973**, *59* (12), 6220−6228.

(24) Rao, R. R.; Kolb, M. J.; Hwang, J.; Pedersen, A. F.; Mehta, A.; You, H.; Stoerzinger, K. A.; Feng, Z.; Zhou, H.; Bluhm, H.; et al. Surface Orientation Dependent Water Dissociation on Rutile Ruthenium Dioxide. *J. Phys. Chem. C* **2018**, *122* (31), 17802−17811.

(25) Guo, Z.; Ambrosio, F.; Chen, W.; Gono, P.; Pasquarello, A. Alignment of Redox Levels at Semiconductor-Water Interfaces. *Chem. Mater.* **2018**, *30* (1), 94−111.

(26) Ambrosio, F.; Guo, Z.; Pasquarello, A. Absolute Energy Levels of Liquid Water. *J. Phys. Chem. Lett.* **2018**, *9* (12), 3212−3216.
(27) Calle-Vallejo, F.; de Morais, R. F.; Illas, F.; Loffreda, D.; Sautet, P. Affordable Estimation of Solvation Contributions to the Adsorption Energies of Oxygenates on Metal Nanoparticles. *J. Phys. Chem. C* **2019**, *123* (9), 5578−5582.
(28) Ledezma-Yanez, I.; Wallace, W. D. Z.; Sebastián-Pascual, P.; Climent, V.; Feliu, J. M.; Koper, M. T. M. Interfacial Water Reorganization as a PH-Dependent Descriptor of the Hydrogen Evolution Rate on Platinum Electrodes. *Nat. Energy* **2017**, *2* (4), 17031.
(29) Sun, K.; Wu, X.; Zhuang, Z.; Liu, L.; Fang, J.; Zeng, L.; Ma, J.; Liu, S.; Li, J.; Dai, R.; et al. Interfacial Water Engineering Boosts Neutral Water Reduction. *Nat. Commun.* **2022**, *13* (1), 6260.
(30) Flyvbjerg, H.; Petersen, H. G. Error Estimates on Averages of Correlated Data. *J. Chem. Phys.* **1989**, *91* (1), 461−466.
(31) Ambrosio, F.; Wiktor, J.; Pasquarello, A. PH-Dependent Surface Chemistry from First Principles: Application to the BiVO 4 (010)-Water Interface. *ACS Appl. Mater. Interfaces* **2018**, *10* (12), 10011−10021.
(32) Siahrostami, S.; Vojvodic, A. Influence of Adsorbed Water on the Oxygen Evolution Reaction on Oxides. *J. Phys. Chem. C* **2015**, *119* (2), 1032−1037.
(33) Karamad, M.; Hansen, H. A.; Rossmeisl, J.; Nørskov, J. K. Mechanistic Pathway in the Electrochemical Reduction of CO 2 on RuO 2. *ACS Catal.* **2015**, *5* (7), 4075−4081.
(34) Feibelman, P. J. Partial Dissociation of Water on Ru(0001). *Science (1979)* **2002**, *295* (5552), 99−102.
(35) Casalongue, H. S.; Kaya, S.; Viswanathan, V.; Miller, D. J.; Friebel, D.; Hansen, H. A.; Nørskov, J. K.; Nilsson, A.; Ogasawara, H. Direct Observation of the Oxygenated Species during Oxygen Reduction on a Platinum Fuel Cell Cathode. *Nat. Commun.* **2013**, *4* (1), 2817.
(36) Tripkovic, V. Thermodynamic Assessment of the Oxygen Reduction Activity in Aqueous Solutions. *Phys. Chem. Chem. Phys.* **2017**, *19* (43), 29381−29388.
(37) He, Z.-D.; Hanselman, S.; Chen, Y.-X.; Koper, M. T. M.; Calle-Vallejo, F. Importance of Solvation for the Accurate Prediction of Oxygen Reduction Activities of Pt-Based Electrocatalysts. *J. Phys. Chem. Lett.* **2017**, *8* (10), 2243−2246.
(38) Zhang, Q.; Asthagiri, A. Solvation Effects on DFT Predictions of ORR Activity on Metal Surfaces. *Catal. Today* **2019**, *323*, 35−43.
(39) Nie, X.; Luo, W.; Janik, M. J.; Asthagiri, A. Reaction Mechanisms of CO2 Electrochemical Reduction on Cu(111) Determined with Density Functional Theory. *J. Catal.* **2014**, *312*, 108−122.
(40) Liu, K.; Cruzan, J. D.; Saykally, R. J. Water Clusters. *Science (1979)* **1996**, *271* (5251), 929−933.
(41) Keutsch, F. N.; Saykally, R. J. Water Clusters: Untangling the Mysteries of the Liquid, One Molecule at a Time. *Proc. Natl. Acad. Sci. U. S. A.* **2001**, *98* (19), 10533−10540.
(42) Di Liberto, G.; Conte, R.; Ceotto, M. Divide-and-Conquer" Semiclassical Molecular Dynamics: An Application to Water Clusters. *J. Chem. Phys.* **2018**, *148* (10), 104302.
(43) Di Liberto, G.; Giordano, L. Role of Solvation Model on the Stability of Oxygenates on Pt(111): A Comparison between Microsolvation, Extended Bilayer, and Extended Metal/Water Interface. *Electrochemical Science Advances* **2023**, DOI: 10.1002/elsa.202100204.
(44) Kresse, G.; Hafner, J. Ab Initio Molecular Dynamics for Liquid Metals. *Phys. Rev. B* **1993**, *47* (1), 558−561.
(45) Kresse, G.; Hafner, J. Ab Initio Molecular-Dynamics Simulation of the Liquid-Metal-Amorphous-Semiconductor Transition in Germanium. *Phys. Rev. B* **1994**, *49* (20), 14251−14269.
(46) Kresse, G.; Furthmüller, J. Efficiency of Ab-Initio Total Energy Calculations for Metals and Semiconductors Using a Plane-Wave Basis Set. *Comput. Mater. Sci.* **1996**, *6* (1), 15−50.
(47) Perdew, J. P.; Burke, K.; Ernzerhof, M. Generalized Gradient Approximation Made Simple. *Phys. Rev. Lett.* **1996**, *77* (18), 3865−3868.
(48) Nosé, S. A Unified Formulation of the Constant Temperature Molecular Dynamics Methods. *J. Chem. Phys.* **1984**, *81* (1), 511−519.
(49) Hoover, W. G. Canonical Dynamics: Equilibrium Phase-Space Distributions. *Phys. Rev. A (Coll Park)* **1985**, *31* (3), 1695−1697.
(50) Ambrosio, F.; Miceli, G.; Pasquarello, A. Structural, Dynamical, and Electronic Properties of Liquid Water: A Hybrid Functional Study. *J. Phys. Chem. B* **2016**, *120* (30), 7456−7470.
(51) Ambrosio, F.; Miceli, G.; Pasquarello, A. Redox Levels in Aqueous Solution: Effect of van Der Waals Interactions and Hybrid Functionals. *J. Chem. Phys.* **2015**, *143* (24), 244508.
(52) Brémond, É.; Savarese, M.; Rega, N.; Ciofini, I.; Adamo, C. Free Energy Profiles of Proton Transfer Reactions: Density Functional Benchmark from Biased Ab Initio Dynamics. *J. Chem. Theory Comput* **2022**, *18* (3), 1501−1511.
(53) Di Liberto, G.; Maleki, F.; Pacchioni, G. PH Dependence of MgO, TiO 2, and γ-Al 2 O 3 Surface Chemistry from First Principles. *J. Phys. Chem. C* **2022**, *126* (24), 10216−10223.
(54) Monteiro, M. C. O.; Dattila, F.; Hagedoorn, B.; García-Muelas, R.; López, N.; Koper, M. T. M. Absence of CO2 Electroreduction on Copper, Gold and Silver Electrodes without Metal Cations in Solution. *Nat. Catal* **2021**, *4* (8), 654−662.
(55) Maleki, F.; Di Liberto, G.; Pacchioni, G. PH- and Facet-Dependent Surface Chemistry of TiO 2 in Aqueous Environment from First Principles. *ACS Appl. Mater. Interfaces* **2023**, *15* (8), 11216−11224.
(56) Grimme, S.; Antony, J.; Ehrlich, S.; Krieg, H. A Consistent and Accurate Ab Initio Parametrization of Density Functional Dispersion Correction (DFT-D) for the 94 Elements H-Pu. *J. Chem. Phys.* **2010**, *132* (15), 154104.
(57) Nørskov, J. K.; Rossmeisl, J.; Logadottir, A.; Lindqvist, L.; Kitchin, J. R.; Bligaard, T.; Jónsson, H. Origin of the Overpotential for Oxygen Reduction at a Fuel-Cell Cathode. *J. Phys. Chem. B* **2004**, *108* (46), 17886−17892.
(58) Atkins, P.; Atkins, P. W.; de Paula, J. *Physical Chemistry*; Oxford University Press: 2014.
(59) Guo, Z.; Ambrosio, F.; Chen, W.; Gono, P.; Pasquarello, A. Alignment of Redox Levels at Semiconductor-Water Interfaces. *Chem. Mater.* **2018**, *30* (1), 94−111.